

西昆仑苦子干新生代透辉石正长岩和透辉石花岗岩 地球化学特征及年代学研究

袁亚娟¹⁾, 陈玮岩²⁾, 夏斌³⁾, 张玉泉⁴⁾, 肖敬国¹⁾, 周厚云¹⁾

1) 华南师范大学地理科学学院, 广州, 510631; 2) 中国石油勘探开发研究院, 北京, 10083;
3) 中山大学海洋学院, 广州, 510275; 4) 中国科学院广州地球化学研究所, 广州, 510640

内容提要:苦子干钾质碱性杂岩体主要由正长岩类和花岗岩类组成, 其中透辉石正长岩主要造岩矿物为钾长石和透辉石, 透辉石花岗岩主要造岩矿物为钾长石、斜长石、石英和透辉石。杂岩体中赋存的透辉石和钙铁辉石, 均属于钙质辉石。两种岩石均属于钾质碱性岩, 具有富碱、高钾、富钙的特征; 富集 Rb、Ba、Th、U 等大离子亲石元素和 Pb, 贫 Nb、Ta、Zr、Hf、Ti 等高场强元素; 稀土元素含量高 ($\Sigma\text{REE} = 372.37 \times 10^{-6} \sim 1218.07 \times 10^{-6}$), 富集轻稀土 ($\text{LREE/HREE} = 21 \sim 37$), 具有轻微的铕负异常 ($\text{Eu/Eu}^* = 0.66 \sim 0.84$)。锆石 U-Pb 定年显示, 透辉石正长岩成岩年龄为 11.7 ± 0.1 Ma, 透辉石花岗岩成岩年龄为 11.0 ± 0.3 Ma, 均属于喜马拉雅期, 相当于中新世末。两类岩石锆石 $\epsilon_{\text{Hf}}(t)$ 范围在 $-9.4 \sim -5.5$ 之间, 介于球粒陨石与下地壳之间。研究表明, 印度大陆与欧亚大陆碰撞, 导致西昆仑-喀喇昆仑地区岩石圈大幅度缩短并加厚, 引发加厚岩石圈拆沉引起软流圈物质上涌底侵, 使得加厚下地壳物质的重熔, 伴随地壳的拉张和抬升, 最终形成苦子干钾质碱性杂岩体。

关键词: 地球化学; 锆石 U-Pb 年龄; 锆石 Hf 同位素; 钾质碱性杂岩体; 苦子干

青藏高原是全球典型的地体碰撞拼贴及隆升区域, 其构造演化一直是地学界的研究热点 (Yin An et al., 2000; Pan Gui Tang et al., 2012; Zhang Kaijun et al., 2014; Wu Fuyuan et al., 2014; Xu Zhiqin et al., 2015)。青藏高原西北部的喀喇昆仑-西昆仑-帕米尔高原地区, 经历了印度板块与欧亚大陆的碰撞、强烈挤压变形等地质事件, 新生代火山活动频繁, 是研究青藏高原演化的关键地区之一 (Zhang Yuquan et al., 1994, 1997; Luo Zhaohua et al., 2003; Jiang Yaohui et al., 2002a, 2002b; Lin Qingcha et al., 2006; Ke Shan et al., 2008; Jiang Yaohui et al., 2012)。位于喀喇昆仑大断裂带上的塔什库尔干碱性杂岩体, 是区内最大的新生代碱性杂岩体。该岩体主要由苦子干杂岩体和卡日巴生岩体组成 (Ke Shan et al., 2006)。其中, 前人对苦子干钾质碱性杂岩体形成时代的测定范围较

大。如正长岩中长石 K-Ar 和花岗岩全岩 K-Ar 年龄分别为 18 Ma 和 33.6 Ma (新疆地质矿产局二大队, 1985); Xu Ronghua et al. (1996) 对辉石正长岩和碱性花岗岩进行钾长石 $^{40}\text{Ar}-^{39}\text{Ar}$ 定年, 分别获得 52Ma 和 17.9 Ma 的坪年龄。Luo Zhaohua et al. (2003) 则测得正长岩和花岗岩的钾长石 $^{40}\text{Ar}-^{39}\text{Ar}$ 坪年龄分别为 13 Ma 和 23 Ma。锆石 U-Pb 定年结果表明, 正长岩年龄为 11.1 Ma 和 10.9 Ma, 花岗岩年龄为 11.3 Ma 和 11.9 Ma (Ke Shan et al., 2008; Wang Yawei et al., 2013)。因此, 苦子干钾质碱性杂岩体的形成年龄尚未准确厘定。而对于苦子干钾质碱性杂岩体的岩浆来源同样存在一定争议, 有待进一步研究讨论。有研究表明苦子干岩体岩浆来源于上地幔, 正长岩和花岗岩属于同源不同阶段的产物 (Zhang Yuquan et al., 1994); Jiang Yaohui et al. (2002a, 2002b) 认为包括苦子干岩类

注: 本文为国家自然科学基金项目(41776056)、广东省自然科学基金项目(2017A030310395)和中国博士后科学基金(2020M672671)资助的成果。

收稿日期: 2019-07-25; 改回日期: 2020-05-20; 网络发表日期: 2020-08-24; 责任编委: 吴才来; 责任编辑: 黄敏。

作者简介: 袁亚娟, 女, 1986 年生, 博士, 特聘副研究员, 主要从事地球化学研究, 邮箱: yuanyajuan@m.scnu.edu.cn。通讯作者: 陈玮岩, 男, 1988 年生, 博士, 工程师, 主要从事地球化学与石油地质研究。邮箱: 7104700@qq.com。

引用本文: 引用本文: 袁亚娟, 陈玮岩, 夏斌, 张玉泉, 肖敬国, 周厚云. 2020. 西昆仑苦子干新生代透辉石正长岩和透辉石花岗岩地球化学特征及年代学研究. 地质学报, 94(10): 2978~2993. doi: 10.19762/j.cnki.dizhixuebao.2020263.

Yuan Yajuan, Chen Weiyan, Xia Bin, Zhang Yuquan, Xiao Jinguo, Zhou Houyun. 2020. Geochemical characteristics and geochronology of the Cenozoic diopside syenite and diopside granite from Kuzigan, Western Kunlun area. Acta Geologica Sinica, 94(10): 2978~2993.

在内的西昆仑造山带喜马拉雅期花岗岩类可能是在板块断离或岩石圈变薄过程中,由俯冲洋壳沉积物的部分熔融或加厚大陆下地壳的交代作用而成; Wang Liankui et al. (2003)根据苦子干岩体 Sr-Nd-Pb 同位素的 EMII 型地幔源区特征,认为岩浆很可能直接来源于钾质富碱地幔; Ke Shan et al. (2006)认为来自于加厚陆壳的下地壳底部镁铁质岩石部分熔融; Jiang Yaohui et al. (2012)通过全岩 Sr-Nd 同位素以及锆石 Hf 同位素数据,揭示苦子干岩体来源于被大陆板片派生熔体交代的脉状岩石圈地幔部分熔融; Wang Yawei et al. (2013, 2017)认为苦子干正长岩是壳幔混合层部分熔融的产物,而花岗岩是地幔热作用以及地壳减压机制下壳源物质再造。为了进一步探讨喀喇昆仑-西昆仑-帕米尔高原的构造-岩浆过程及其在青藏高原演化中的意义,本文选取苦子干钾质碱性杂岩体中的正长岩和花岗岩进行矿物化学、全岩地球化学、锆石 U-Pb 定年和锆石 Hf 同位素地球化学等方面的研究,以期进一步厘定其形成时代,探讨其源区特征及其他地质意义。

1 地质背景与岩相学

苦子干钾质碱性杂岩体是哀牢山-金沙江新生代钾质碱性岩浆岩带中众多的钾质碱性岩体之一(图 1a, Zhang Yuquan et al., 1997)。哀牢山-金沙江新生代碱性钾质岩浆岩带,长约 3700 km,呈 NW 向连续分布,到玉树西南杂多转为 NWW 向,沿北纬 35°~36°之间,向南到金平经可可西里继续向西延展到新疆西南部塔什库尔干一带,在成岩时代上具有东早西晚的特征(Zhang Yuquan et al., 1987)。前人对该带钾质碱性岩浆岩开展过大量研究,积累了众多的同位素定年数据,该类岩石成岩年龄范围在 41~3 Ma(Arnaud et al., 1992; Zhang Yuquan et al., 1997; Williams et al., 2004; Hou Zengqian et al., 2011; Xu Leiluo et al., 2012; Lu Yongjun et al., 2013; Yuan Yajuan et al., 2013; Guo Zhengfu et al., 2014; Tran et al., 2014; Xia Bin et al., 2018)。岩浆活动起始时间略晚于印度与欧亚两大陆初始碰撞时间(45±5) Ma (Zhong Dalai et al., 1996; Xia Bin et al., 2009; Dai Jingen et al., 2013; Wang Erchie et al., 2015)。

苦子干钾质碱性杂岩体位于塔什库尔干县城以西约 7 km,岩体南北长约 32 km,东西宽约 5~8 km,面积约为 190 km²。岩体西侧侵入于二叠纪地层中,接触面内倾,倾角 70°,东界被第四系覆盖。

其中透辉石花岗岩侵入于透辉石正长岩中(见 A-A'),显示环状复式岩体特点(图 1b, 新疆地质矿产局二大队, 1985)。

本文在沟口-斯如依迭尔沟剖面分别采集透辉石正长岩和透辉石花岗岩样品各 4 件。岩石薄片磨制在中国科学院广州地球化学研究所完成,并在尼康 ECLIPSE LV100POL 偏光显微镜下进行薄片鉴定与照相。样品 KS3 镜下定名为透辉石正长岩,岩石呈褐灰色,中-粗粒结构、等粒结构,局部可见似斑状结构,块状构造(图 2a)。其主要造岩矿物有钾长石(30%~50%)、斜长石(5%~30%)、透辉石(10%~30%)、石英(0~5%),副矿物有磁铁矿、萤石、磷灰石和锆石等矿物。样品 KG2 镜下定名为透辉石花岗岩,岩石呈肉红色-微红色,中细粒等粒结构,块状构造(图 2b)。主要造岩矿物为钾长石(30%~35%)、斜长石(30%~35%)、石英(~20%)、透辉石(~5%),还含有少量的磁铁矿、萤石、榍石、磷灰石和锆石等矿物。

2 分析方法

2.1 单矿物辉石电子探针分析

辉石电子探针分析在中国地质科学院矿产资源研究所电子探针实验室完成。实验条件为: 加速电压 15 keV, 探针电流 2×10^{-8} A, 束斑直径 $< 1 \mu\text{m}$; 定量分析的标样为美国国家标准局的矿物标样, 其中 SiO₂、TiO₂、Al₂O₃、FeO、MgO、CaO、Na₂O 和 K₂O 使用角闪石为标样, MnO 使用铁橄榄石为标样。

2.2 全岩地球化学分析

样品全岩主量元素在中国科学院广州地球化学研究所 Rigaku RIX 2000 型 X 射线荧光光谱仪(XRF)中完成,分析精度优于 5%。微量元素包括稀土元素,在中国科学院广州地球化学研究所同位素地球化学国家重点实验室用 PE-Elan 6000 型 ICP-MS 测试,元素误差小于 5%。主量元素和微量元素的分析流程参照 Li Xianhua et al. (2005) 和 Liu Yin et al. (1996)。

2.3 锆石 U-Pb 定年

透辉石正长岩样品 KS3 的 U-Pb LA-ICP-MS 定年在中国科学院广州地球化学研究所同位素地球化学国家重点实验室完成。实验仪器为 Resolution M-50 激光剥蚀系统和 Agilent 7500a 型的 ICP-MS 联机,激光剥蚀斑束直径为 31 μm,频率为 8 Hz,锆石剥蚀过程中采用 He 气作为剥蚀物质的载气。采用单点剥蚀的方法。元素含量外标采用美国国家标

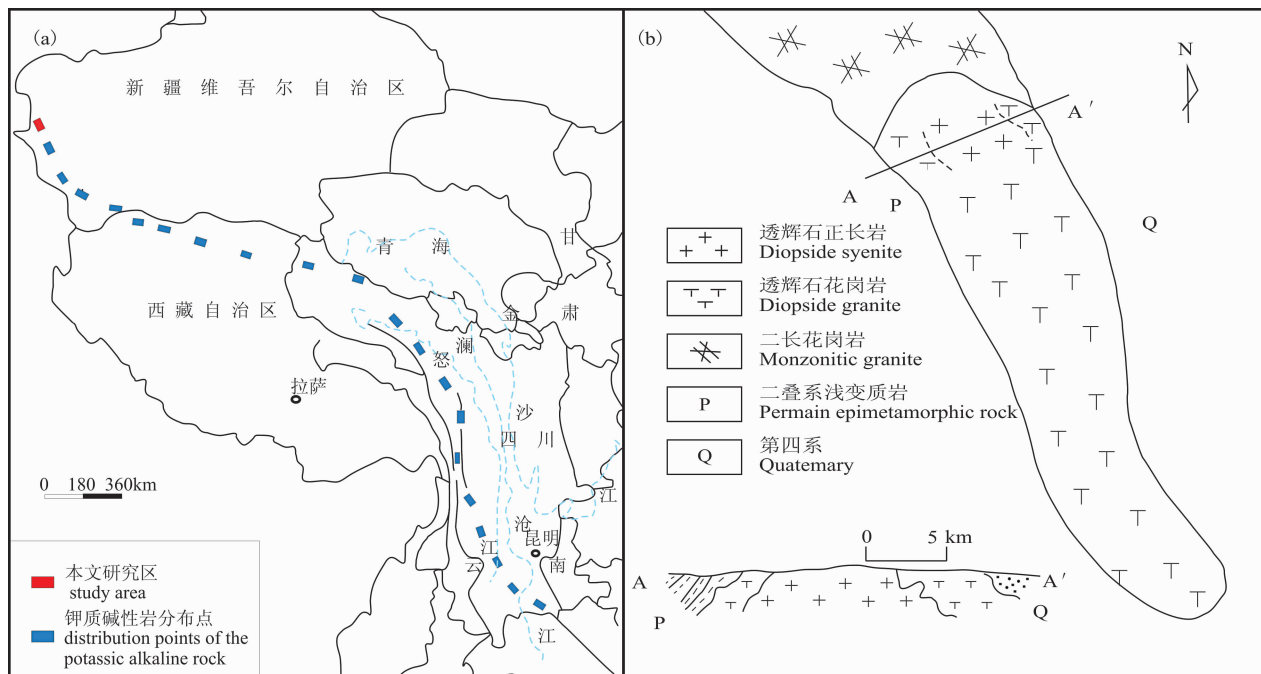


图 1 哀牢山-金沙江钾质碱性岩体分布示意图(a)和苦子干钾质碱性杂岩体地质图(b)

Fig. 1 Schematic map showing the distribution of alkali-rich intrusive bodies in the Ailaoshan-Jinshajiang belt (a) and geological map of Kuzigan potassio alkaline complex mass (b)

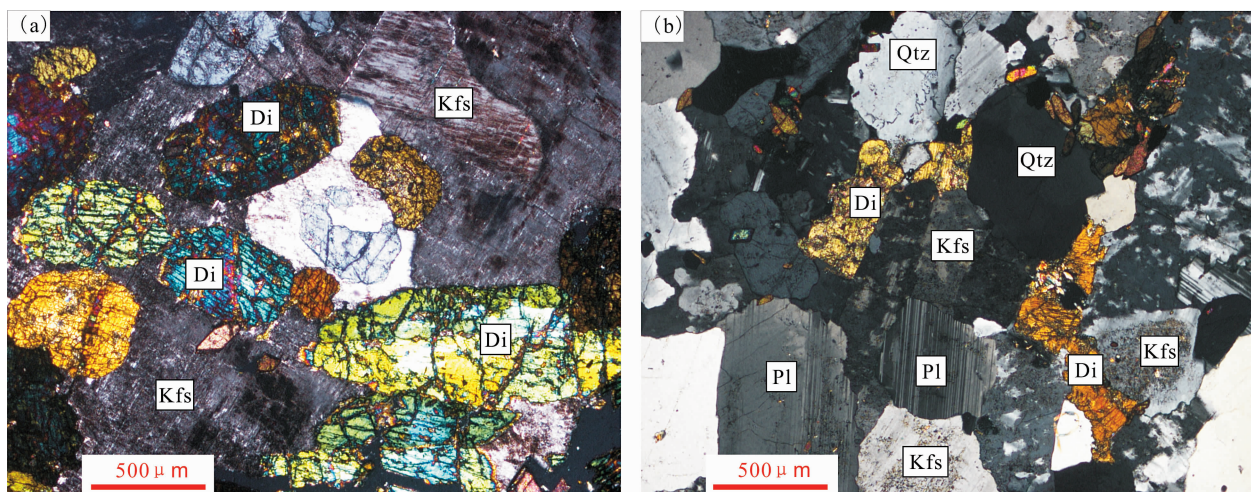


图 2 西昆仑苦子干透辉石正长岩(a)、透辉石花岗岩(b)镜下特征(正交偏光)

Fig. 2 Microscopic characteristics of the diopside syenite (a) and diopside granite (b)

(orthogonal polarized light) in western Kunlun

Kfs—钾长石; Di—透辉石; Pl—斜长石; Qtz—石英

Kfs—Potassium feldspar; Di—diopside; Pl—plagioclase; Qtz—quartz

准技术研究院人工合成的硅酸盐玻璃标准参考物质 NIST610, 元素内标采用²⁹Si, 锆石年龄外标则采用 Temora (417 Ma)。详细的实验流程和参数设置见 Li Congying et al. (2012)。测得的激光信号数据使用 ICPMSData 7.2 软件进行处理 (Liu Yongsheng et al., 2008), 并利用 Andersen (2002) 的方法进行普通 Pb 校正, 获得可靠的锆石微量元素含量和 U-

Pb 同位素比值, 最终通过 Isoplot 3.15 软件计算出样品的 U-Pb 年龄谐和图和加权平均年龄 (Ludwing, 2003)。

透辉石花岗岩样品 KG2 的 U-Pb SHRIMP 定年在中国地质科学院地质研究所北京离子探针中心完成。本次定年采用 SL13 (572 Ma, U = 238 × 10⁻⁶) 做为锆石微量元素外标 (Williams et al.,

1996), 年龄外标则同样选择 Temora ($^{206}\text{Pb}/^{238}\text{U}$ 年龄 = 417 Ma) (Black et al., 2003), 详细的仪器操作和测试步骤参考 Jian Ping et al. (2012), 普通 Pb 校正参考 Compston et al. (1992), U-Pb 年龄谱和图和加权平均年龄的计算通过 Isoplot 3.15 软件完成 (Ludwing, 2003)。

锆石样品的原位 Lu-Hf 同位素测定在中国科学院广州地球化学研究所同位素地球化学国家重点实验室完成。实验设备为 RESolution M-50 型 193nmArF 准分子激光剥蚀系统和 Neptune Plus 型多接收等离子质谱(MC-ICP-MS)。激光剥蚀斑束直径为 45 μm , 剥蚀频率 8 Hz, 采用 He 气作为剥蚀物质载气, 每个样点测试总时长约 60 s, 其中约 30 s 为剥蚀时间。具体的仪器设置和分析流程可参考 Zhang Yuxiu et al. (2015)。本次测试采用 Penglai 锆石为外标。全过程中测得的 Penglai 锆石 $^{176}\text{Hf}/^{177}\text{Hf} = 0.282901 \pm 0.000005$ ($\pm 2\sigma, n=12$), 与文献 Li Xianhua et al. (2010) 中的推荐值 ($^{176}\text{Hf}/^{177}\text{Hf} = 0.282906 \pm 0.000010$) 一致。测试数据获得后, 采用标准值 $^{179}\text{Hf}/^{177}\text{Hf} = 0.7325$ 对样品 $^{176}\text{Hf}/^{177}\text{Hf}$ 值进行质量分馏校正, 而 ^{176}Lu 和

^{176}Yb 对 ^{176}Hf 的同质异位干扰则分别使用 $^{176}\text{Lu}/$

$^{175}\text{Lu} = 0.02655$ 和 $^{176}\text{Yb}/^{171}\text{Yb} = 0.90184$ 来进行校正(Patchett et al., 1981; Blichert et al., 1997; Nowell et al., 1998)。

3 分析结果

3.1 辉石矿物化学

对苦子干透辉石正长岩和透辉石花岗岩中的辉石进行电子探针分析, 并将分析结果以 6 个氧为基础, 计算阳离子系数, 数据如表 1 所列。结果表明, 苦子干钾质碱性杂岩体中的辉石 ΣCa 含量较高, 达到 18.75% ~ 21.23%; ΣNa 含量则较低, $\Sigma\text{Na}_2\text{O}$ 在 0.9% ~ 2.9% 之间, 均表现为富钙(Ca)、贫钠(Na)的特点。在 Q-J 图解中(图 3a), 样品均落入辉石四角边区 Quad(Ca-Mg-Fe 辉石组)。在 Wo-En-Fs 图解中(图 3b), 正长岩数据点均落入透辉石区, 而花岗岩有两个辉石成分点落入钙铁辉石区, 另外两个则落入透辉石区(Morimoto, 1988)。这表明苦子干杂岩体中, 无论是中性的透辉石正长岩, 还是酸性的透辉石花岗岩, 其赋存的辉石(透辉石和钙铁辉石)均为钙质辉石。

3.2 元素地球化学特征

样品全岩主量和微量元素结果见表 2。透辉石

表 1 西昆仑苦子干钾质碱性杂岩体辉石电子探针(%)分析结果

Table 1 Electron probe (%) of the pyroxenes for Kuzigan potassic alkaline complex mass in western Kunlun

岩性	透辉石正长岩							透辉石花岗岩			
	KS1 _a	KS1 _b	KS1 _c	KS1 _d	KS1 _e	KS1 _f	KS1 _g	KG1 _a	KG1 _b	KG1 _c	KG1 _d
SiO ₂	53.02	52.95	53.01	54.06	52.76	53.02	52.73	52.87	52.34	53.53	52.12
TiO ₂	0.53	0.48	0.41	0.11	0.10	0.53	0.09	0.09	0.02	0.04	0.11
Al ₂ O ₃	1.22	0.79	0.77	0.64	0.70	1.22	0.66	0.66	0.46	0.35	0.82
FeO	9.60	8.56	9.54	11.36	14.29	9.60	13.86	13.86	17.84	12.86	15.05
MnO	0.23	0.22	0.27	0.26	0.42	0.23	0.69	0.69	1.19	1.04	0.83
MgO	13.09	12.86	12.46	11.78	9.74	13.09	9.13	9.13	6.24	10.24	8.70
CaO	20.99	21.23	21.05	19.22	18.78	20.99	19.92	19.92	19.19	20.05	20.78
Na ₂ O	1.04	0.97	0.92	2.46	2.90	1.04	1.23	1.23	1.57	1.30	0.90
K ₂ O	—	—	0.03	—	—	—	—	—	—	—	0.01
Cr ₂ O ₃	—	—	—	0.10	0.03	0.02	0.09	—	—	—	—
Total	99.72	98.06	98.46	99.99	99.72	99.74	98.40	98.45	98.85	99.41	99.32
Si	1.98	2.01	2.01	2.01	1.99	1.98	2.05	2.05	2.06	2.04	2.02
Ti	0.02	0.01	0.01	0.00	0.00	0.02	0.00	0.00	0.00	0.00	0.00
Al	0.03	0.04	0.03	0.03	0.02	0.04	0.03	0.03	0.02	0.02	0.04
Fe	0.19	0.22	0.25	0.19	0.23	0.20	0.44	0.44	0.59	0.40	0.46
Mn	0.01	0.01	0.01	0.01	0.01	0.01	0.02	0.02	0.04	0.03	0.03
Mg	0.73	0.73	0.71	0.65	0.55	0.73	0.53	0.53	0.37	0.58	0.50
Ca	0.84	0.86	0.86	0.77	0.76	0.84	0.83	0.83	0.81	0.82	0.86
Na	0.08	0.07	0.07	0.18	0.21	0.07	0.09	0.09	0.12	0.10	0.07
K	—	—	0.00	—	—	—	—	—	—	—	—
Wo	44.80	46.20	45.70	43.00	42.90	44.80	45.30	45.30	44.90	44.40	45.90
En	38.90	38.90	37.70	36.70	30.90	38.90	28.90	28.90	20.30	31.60	26.70
Fs	16.40	14.90	16.60	20.30	26.20	16.40	25.80	25.80	34.80	24.00	27.40

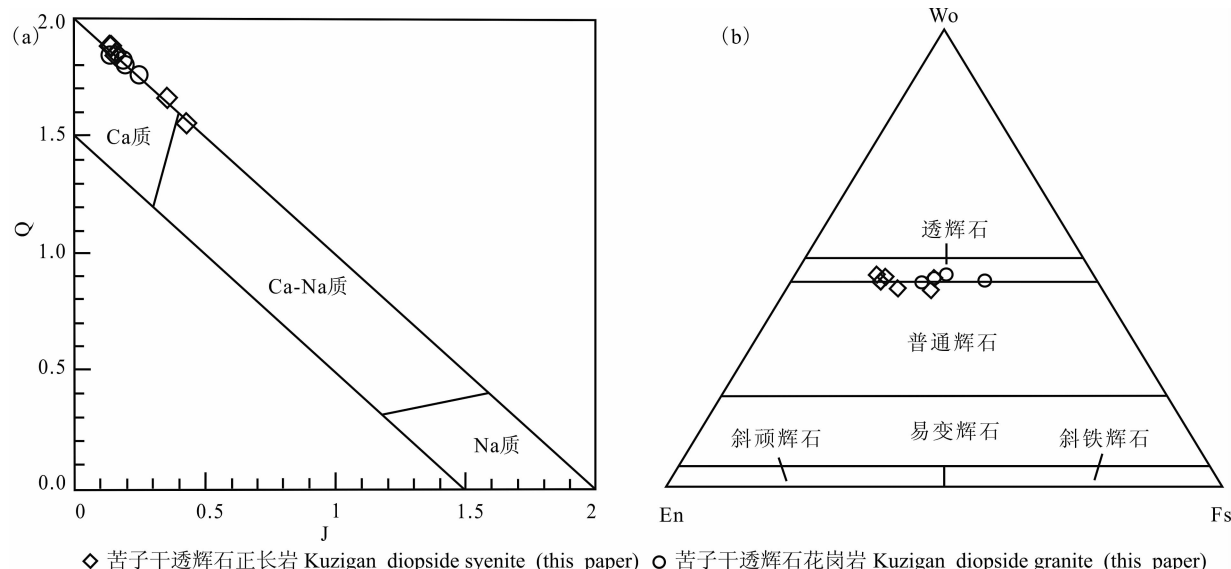


图 3 西昆仑苦子干钾质碱性杂岩体辉石的 Q-J 图解(a)和 Wo-En-Fs 图解(b)(据 Morimoto, 1988)

Fig. 3 Q-J diagram (a) and Wo-En-Fs diagram (b) of pyroxenes in Kuzigan potassio alkaline complex mass (after Morimoto, 1988) in western Kunlun

正长岩 SiO_2 含量变化在 57.1%~61.2% 之间, 总碱 ($\text{Na}_2\text{O} + \text{K}_2\text{O}$) 含量变化在 9.12%~12.55% 之间, $\text{Na}_2\text{O}/\text{K}_2\text{O}$ 变化在 0.39~0.51 之间, Al_2O_3 含量变化在 11.13%~15.78% 之间, CaO 含量变化在 3.36%~9.77% 之间; 透辉石花岗岩 SiO_2 含量变化在 70.70%~71.04% 之间, 总碱 ($\text{Na}_2\text{O} + \text{K}_2\text{O}$) 含量变化于 9.36%~10.04% 之间, $\text{Na}_2\text{O}/\text{K}_2\text{O}$ 变化在 0.62~0.76 之间, CaO 含量变化在 1.62%~1.72% 之间, Al_2O_3 含量变化于 13.53%~14.69% 之间, 铝饱和指数 A/CNK 值变化在 0.84~0.93, 属于准铝质花岗岩。透辉石正长岩和透辉石花岗岩在岩石化学成分上均表现为富碱、高钾和富钙的特征。

根据 Wright(1969) 的 SiO_2 -AR 图解分析方法, 投图可见数据点均分布在碱性区(图 4a)。再根据 Irvine 和 Barager(1971) 的 An-Ab-Or 图解(图 4b), 对数据点进行投图, 均处在钾质区, 表明苦子干正长岩和花岗岩均属于钾质碱性岩, 与前人认识一致 (Jiang Yaohui et al., 2002a; Ke Shan et al., 2006; Jiang Yaohui et al., 2012; Wang Yawei et al., 2013)。

透辉石正长岩稀土元素含量变化范围为 649.83×10^{-6} ~ 1218.07×10^{-6} , 富集轻稀土元素 ($\text{LREE/HREE}=20.83\sim26.34$), 钇呈现轻微负异常 ($\text{Eu/Eu}^*=0.74\sim0.84$), 稀土模式为右倾斜 LREE 富集型 ($\text{La/Yb}_N=53.7\sim66.2$) (图 5a)。透

辉石花岗岩稀土元素含量变化范围为 372.37×10^{-6} ~ 696.59×10^{-6} , 富集轻稀土元素 ($\text{LREE/HREE}=24.74\sim37.36$), 钇较弱负异常 ($\text{Eu/Eu}^*=0.66\sim0.82$), 稀土模式为右倾斜 LREE 富集型 ($\text{La/Yb}_N=57\sim80$) (图 5a)。此外, 反映 LREE 分馏程度的 $(\text{La}/\text{Sm})_N$ 参数整体在 4.47~11.9 范围之间, 反映 HREE 分馏程度的 $(\text{Gd}/\text{Yb})_N$ 在 2.56~6.13 范围之间, 显示岩浆岩体的轻重稀土均发生一定程度的轻度分馏, 轻稀土元素的分馏程度大于重稀土元素。两类岩石的微量元素蛛网图均表现出富集 Rb、Ba、Th、U、Sr 等大离子亲石元素和富 Pb, 贫 Nb、Ta、Zr、Hf、Ti 等高场强元素的特征 (图 5b)。

3.3 锆石 U-Pb 年龄

通过锆石透反射及阴极发光照片(图 6)对比, 选择晶形形态完整、内部结构较为清晰且具震荡环带发育的锆石颗粒, 在无包裹体或杂质的干净部位进行打点测试。锆石 LA-ICP-MS 和 SHRIMP U-Pb 分析结果见表 3。

透辉石正长岩样品 KS3 锆石多为不规则的自形晶体, 粒径长在 100~400 μm 不等, 环带发育。实验共测定 17 个点, Th 的含量变化范围为 216×10^{-6} ~ 6646×10^{-6} , U 的含量变化范围为 330×10^{-6} ~ 5995×10^{-6} , Th/U 的比值范围是 0.44~1.47, 将谐和度低于 80% 的数据剔除, $^{206}\text{Pb}/^{238}\text{U}$ 加权平均年龄为 $11.7 \pm 0.1 \text{ Ma}$ ($\text{MSWD}=0.77, n=10$), 为岩体的侵位结晶年龄(图 7a)。

表 2 西昆仑苦子干钾质碱性杂岩体全岩主量(%)和微量元素($\times 10^{-6}$)分析结果Table 2 Representative composition of major(%) and trace element ($\times 10^{-6}$) contents in alkaline rocks within Kuzigan potassic alkaline complex mass in western Kunlun

序号*	1	2	3	4	5	6	7	8
样号	KS1	KS2	KS3	KS4	KG1	KG2	KG3	KG4
SiO ₂	57.10	57.30	61.08	61.20	71.04	70.70	70.73	70.80
TiO ₂	0.92	0.90	0.82	0.82	0.23	0.19	0.29	0.25
Al ₂ O ₃	11.13	11.50	15.78	15.55	13.53	13.55	14.69	14.25
Fe ₂ O _{3T}	6.44	6.38	3.58	4.18	2.04	2.41	1.92	2.25
MnO	0.19	0.19	0.11	0.12	0.08	0.09	0.06	0.06
MgO	3.09	2.75	0.85	0.90	0.28	0.21	0.22	0.30
CaO	9.77	8.30	3.39	3.36	1.72	1.62	1.63	1.64
Na ₂ O	3.10	3.12	3.57	3.42	3.84	3.79	4.01	4.03
K ₂ O	6.02	6.44	8.98	8.83	6.20	5.95	5.58	5.33
P ₂ O ₅	0.71	0.83	0.15	0.15	0.02	0.04	0.05	0.05
LOI	0.68	0.74	0.56	0.45	0.49	0.52	0.33	0.33
总量	99.15	98.45	98.87	98.98	99.47	99.07	99.51	99.29
Na ₂ O+K ₂ O	9.12	9.56	12.55	12.25	10.04	9.74	9.59	9.36
Na ₂ O/K ₂ O	0.51	0.48	0.40	0.39	0.62	0.64	0.72	0.76
AR	2.55	2.87	4.79	4.68	4.85	4.59	3.85	3.87
微量元素								
Sc	12.20	11.50	5.64	4.30	2.05	1.30	3.71	1.90
Ti	5520	4920	5400	4920	1380	1740	1140	1500
V	104.00	102.00	66.00	72.00	28.10	27.00	23.30	21.00
Cr	71.20	60.00	31.40	30.00	14.80	10.00	17.10	10.00
Co	13.40	10.10	5.68	5.30	1.85	1.60	1.81	1.50
Ni	33.00	22.50	12.00	9.10	5.70	2.70	5.79	4.40
Cu	8.15	10.90	29.80	27.90	3.64	4.30	11.00	8.60
Zn	184.00	143.00	90.50	74.00	39.20	33.00	33.90	22.00
Ga	19.70	19.50	23.20	24.20	22.70	22.50	21.80	22.60
Ge	2.21	0.61	1.49	0.54	1.36	0.37	1.39	0.45
Rb	320	336	337	435	311	304	289	282
Sr	2310	2310	2530	2470	1740	1675	1320	1286
Y	53.68	47.10	32.80	31.80	15.13	14.20	26.06	23.30
Zr	232	416	378	429	453	494	385	407
Nb	22.00	26.30	32.20	33.50	20.20	20.30	23.00	22.00
Cs	4.64	4.75	5.87	5.74	5.54	5.51	7.01	6.05
Ba	3060	2970	2760	3560	2350	2310	2190	1910
Hf	7.46	10.10	8.97	10.40	10.30	12.20	10.80	10.20
Ta	1.83	1.60	1.94	1.70	0.82	0.80	1.32	0.90
Pb	77.50	62.40	47.90	45.90	63.00	65.80	45.70	40.60
U	4.47	5.55	5.87	9.94	12.60	14.00	16.20	18.70
Th	50.40	48.90	45.60	66.20	65.80	73.60	88.80	114.50
La	269	309	172	172	126	122	205	213
Ce	489.00	555.00	261.00	339.00	152.00	188.50	270.00	333.00
Pr	66.20	59.80	35.60	37.70	18.20	18.65	32.70	30.10
Nd	238.00	209.00	127.00	131.50	56.20	58.20	104.00	88.50
Sm	38.90	33.60	21.20	21.80	7.56	8.13	14.50	11.55
Eu	7.67	7.12	4.33	4.60	1.43	1.65	2.72	2.28
Gd	25.78	21.00	12.90	13.00	4.51	4.71	11.14	6.88
Tb	2.78	2.47	1.55	1.58	0.54	0.58	1.15	0.92
Dy	12.50	10.95	7.19	7.31	2.55	2.83	5.55	4.31
Ho	2.14	1.77	1.26	1.20	0.49	0.49	1.05	0.81
Er	5.33	3.94	3.08	2.77	1.38	1.38	3.10	2.29
Tm	0.62	0.57	0.37	0.35	0.19	0.20	0.41	0.38
Yb	3.48	3.35	2.02	2.30	1.13	1.30	2.58	2.22

续表 2

序号*	1	2	3	4	5	6	7	8
样号	KS1	KS2	KS3	KS4	KG1	KG2	KG3	KG4
Lu	0.60	0.50	0.33	0.30	0.19	0.21	0.44	0.35
TREE	1162.00	1218.07	649.83	735.41	372.37	408.33	654.34	696.59
LREE/HREE	20.83	26.34	21.64	24.53	32.91	33.90	24.74	37.36
Eu/Eu *	0.74	0.82	0.80	0.84	0.75	0.82	0.66	0.78
La/Yb	55.47	66.19	61.10	53.66	80.02	67.07	57.02	68.85
La/Sm	4.47	5.94	5.24	5.10	10.77	9.66	9.14	11.92

注: AR = $(\text{Al}_2\text{O}_3 + \text{CaO} + \text{Na}_2\text{O} + \text{K}_2\text{O}) / (\text{Al}_2\text{O}_3 + \text{CaO} + \text{Na}_2\text{O} + \text{K}_2\text{O})$, $\delta\text{Eu} = \text{Eu}_{\text{N}} / (\text{Sm}_{\text{N}} \times \text{Gd}_{\text{N}})^{1/2}$ 。

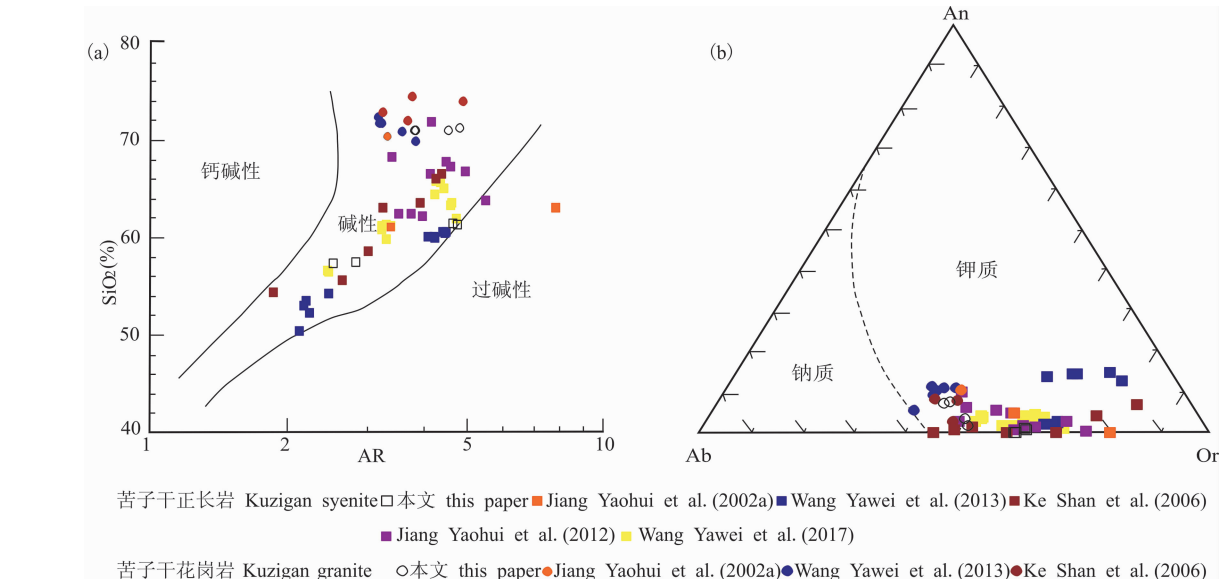


图 4 西昆仑苦子干钾质碱性杂岩体的 SiO_2 -AR 图解(a) (据 Wright, 1969) 和 Ab-An-Or 图解(b) (据 Irvine et al., 1971)

Fig. 4 SiO_2 -AR diagram(a) (after Wright, 1969) and Ab-An-Or diagram(b) (after Irvine et al., 1971)
of Kuzigan potassio-alkaline complex in western Kunlun

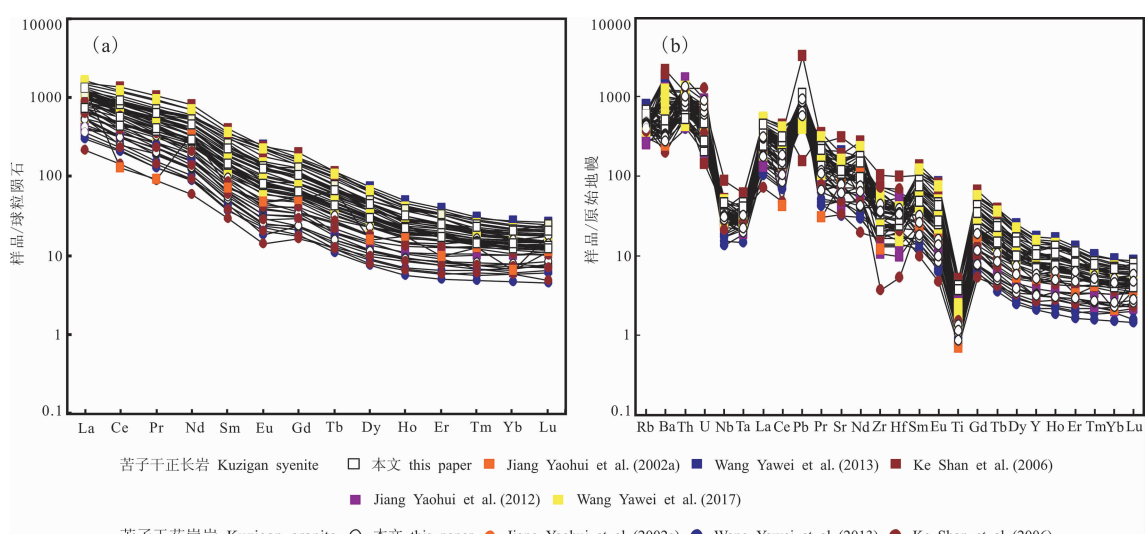


图 5 西昆仑苦子干钾质碱性杂岩体稀土元素球粒陨石标准化图解和原始地幔标准化不相容元素配分图解
(标准化值据 Sun et al., 1989)

Fig. 5 Chondrite-normalized REE patterns and primitive mantle-normalized patterns of incompatible elements
of Kuzigan potassio-alkaline complex mass in western Kunlun (normalized data after Sun et al., 1989)

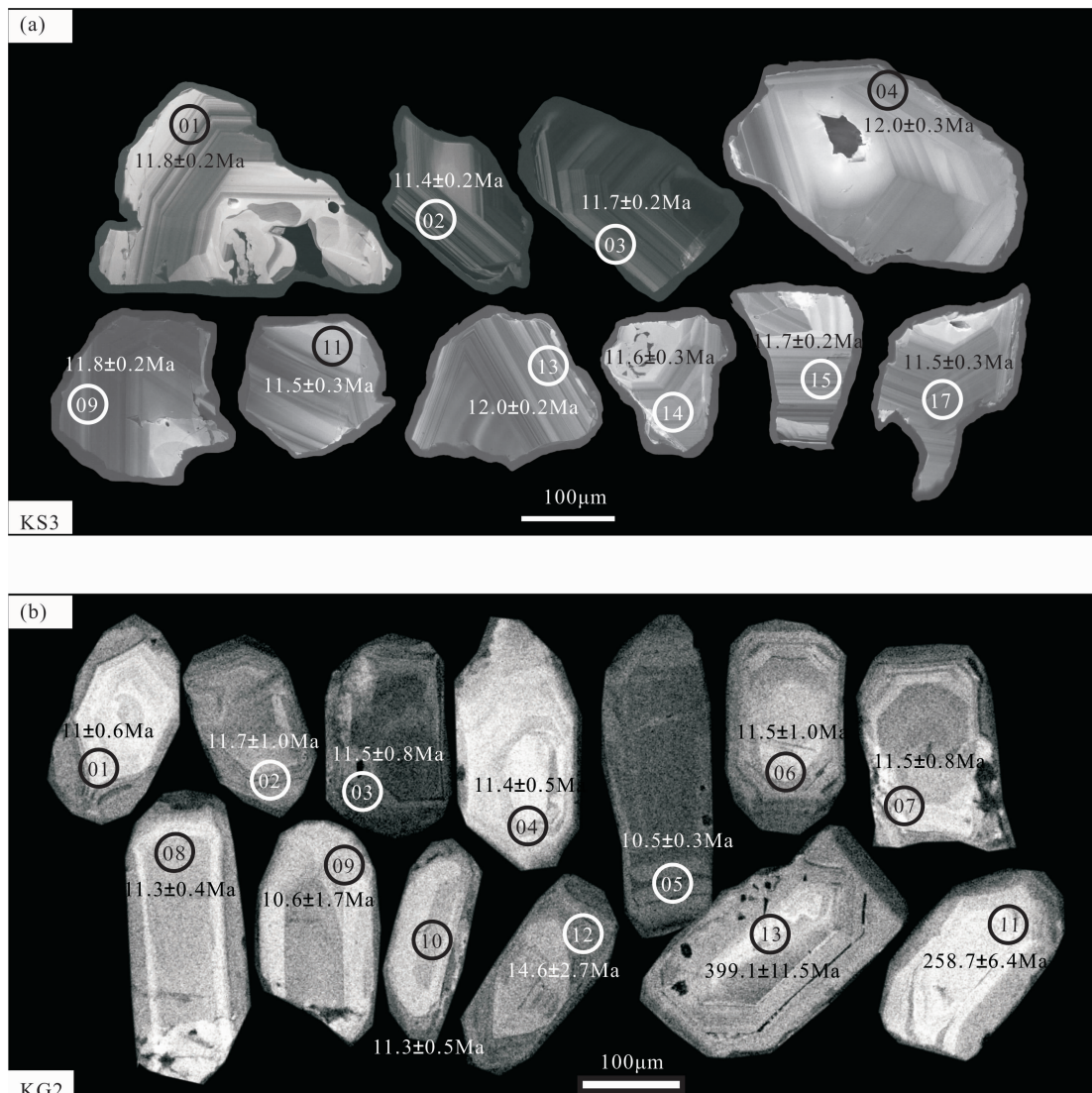


图 6 西昆仑苦子干透辉石正长岩(a)和透辉石花岗岩(b)锆石阴极发光(CL)图像及测试位置

Fig. 6 Cathodoluminescence images and sampling position of zircons from Kuzigan diopside syenite (a) and diopside granite (b) in western Kunlun

透辉石花岗岩样品 KG2 锆石多为自形程度较好的长柱状晶体,粒径长在 250~300 μm 之间,环带发育,岩浆锆石特征明显。实验共测定 13 个点,Th 的含量变化范围为 $13 \times 10^{-6} \sim 607 \times 10^{-6}$,U 的含量变化范围为 $130 \times 10^{-6} \sim 891 \times 10^{-6}$,Th/U 的比值范围是 0.03~1.27,平均为 0.66,除去两个继承锆石年龄数据(KG2-11、KG2-13), $^{206}\text{Pb}/^{238}\text{U}$ 加权平均年龄为 11.0 ± 0.3 Ma(MSWD=0.75,n=11),代表岩体的侵位结晶年龄(图 7b)。两类岩石的成岩年龄与它们之间的侵入接触关系相一致。

3.4 锆石原位 Hf 同位素

由于苦子干钾质碱性杂岩体中透辉石正长岩和透辉石花岗岩的锆石 $^{176}\text{Lu}/^{177}\text{Hf}$ 比值范围为 0.000205~0.001673,均小于 0.002,表明锆石在形

成之后没有明显的放射性成因 Hf 的积累(Wu Fuyuan et al., 2007)。透辉石正长岩样品 KS3 锆石 $^{176}\text{Hf}/^{177}\text{Hf}$ 比值在 0.282525~0.282610 之间, $f_{\text{Lu/Hf}}$ 值范围在 -0.99~-0.95 之间。各点根据岩石成岩的谐和年龄校正计算后 $\epsilon_{\text{Hf}}(t)$ 值范围为 -8.5~-5.5,样品 Hf 二阶段模式年龄(T_{DM2})集中于 1.45~1.64 Ga 之间。

透辉石花岗岩样品 KG2 锆石 $^{176}\text{Hf}/^{177}\text{Hf}$ 比值在 0.282506~0.282572 之间, $f_{\text{Lu/Hf}}$ 值范围在 -0.99~-0.96。根据锆石 U-Pb 定年的谐和年龄校正计算后得出 $\epsilon_{\text{Hf}}(t)$ 值均为不同程度的负值,分布于 -9.2~-6.8 之间,样品 Hf 二阶段模式年龄(T_{DM2})集中于 1.53~1.68 Ga 之间。

表 3 西昆仑苦子干钾质碱性杂岩体锆石 U-Pb 年龄数据

Table 3 Zircon U-Pb dating results of Kuzigan potassio alkaline complex mass in western Kunlun

测点	含量($\times 10^{-6}$)			Th/U	同位素比值						年龄(Ma)	
	Pb	Th	U		$^{207}\text{Pb}/^{206}\text{Pb}$	$\pm 1\sigma$	$^{207}\text{Pb}/^{235}\text{U}$	$\pm 1\sigma$	$^{206}\text{Pb}/^{238}\text{U}$	$\pm 1\sigma$	$^{206}\text{Pb}/^{238}\text{U}$	$\pm 1\sigma$
透辉石正长岩												
KS3-01	4.31	2235.15	1593.41	1.40	0.04840	0.00271	0.01231	0.00070	0.00184	0.00004	11.8	0.2
KS3-02	5.89	2632.59	2426.51	1.08	0.04510	0.00210	0.01107	0.00052	0.00177	0.00003	11.4	0.2
KS3-03	6.63	3564.06	2418.80	1.47	0.04339	0.00196	0.01097	0.00053	0.00182	0.00003	11.7	0.2
KS3-04	1.27	355.67	556.35	0.64	0.04686	0.00361	0.01178	0.00085	0.00187	0.00005	12.0	0.3
KS3-05 *	2.16	773.02	839.37	0.92	0.05994	0.00483	0.01527	0.00124	0.00185	0.00004	11.9	0.3
KS3-06 *	9.88	1415.11	3197.82	0.44	0.10087	0.00970	0.03104	0.00358	0.00217	0.00004	13.9	0.3
KS3-07 *	5.95	871.09	954.16	0.91	0.22790	0.03313	0.14811	0.03289	0.00297	0.00029	19.1	1.8
KS3-08 *	30.82	6645.71	5995.02	1.11	0.13901	0.02146	0.06567	0.01553	0.00234	0.00015	15.1	1.0
KS3-09	2.56	941.20	988.61	0.95	0.05669	0.00334	0.01417	0.00082	0.00183	0.00003	11.8	0.2
KS3-10 *	0.78	215.74	329.94	0.65	0.07468	0.00949	0.01732	0.00186	0.00178	0.00005	11.5	0.4
KS3-11	2.44	1045.62	1000.40	1.05	0.04535	0.00232	0.01115	0.00062	0.00179	0.00004	11.5	0.3
KS3-12 *	3.38	750.54	940.63	0.80	0.13492	0.01596	0.04730	0.00692	0.00221	0.00008	14.2	0.5
KS3-13	2.85	1160.83	1112.85	1.04	0.04263	0.00230	0.01083	0.00057	0.00186	0.00004	12.0	0.2
KS3-14	1.54	485.92	655.45	0.74	0.05295	0.00537	0.01275	0.00125	0.00181	0.00004	11.6	0.3
KS3-15	2.93	1137.15	1185.06	0.96	0.05084	0.00301	0.01270	0.00076	0.00181	0.00004	11.7	0.2
KS3-16 *	3.03	1269.72	1102.21	1.15	0.05986	0.00588	0.01603	0.00194	0.00188	0.00004	12.1	0.3
KS3-17	2.25	910.33	943.68	0.96	0.04625	0.00362	0.01122	0.00087	0.00178	0.00004	11.5	0.3
透辉石花岗岩												
KG2-01	1.20	161	424	0.37	0.21050	0.00130	0.06260	0.00046	0.00190	0.00001	11.0	0.6
KG2-02	0.90	355	280	1.27	0.13450	0.00490	0.02910	0.00099	0.00180	0.00002	11.7	1.0
KG2-03	0.80	304	266	1.14	0.12170	0.00280	0.02850	0.00067	0.00180	0.00001	11.5	0.8
KG2-04	1.20	226	537	0.42	0.04930	0.00170	0.01200	0.00040	0.00180	0.00001	11.4	0.5
KG2-05	2.10	607	891	0.68	0.06070	0.00740	0.01330	0.00016	0.00160	0.00001	10.5	0.3
KG2-06	0.50	167	168	0.99	0.13470	0.00710	0.02470	0.00101	0.00180	0.00001	11.5	0.8
KG2-07	0.40	104	130	0.80	0.09510	0.00130	0.08280	0.00177	0.00180	0.00002	11.5	1.0
KG2-08	1.10	348	453	0.77	0.10640	0.00300	0.02380	0.00061	0.00180	0.00001	11.3	0.4
KG2-09	0.80	253	236	1.07	0.30340	0.00980	0.06850	0.00218	0.00160	0.00003	10.6	1.7
KG2-10	1.20	317	494	0.64	0.07190	0.00170	0.01590	0.00461	0.00170	0.00001	11.3	0.5
KG2-11 *	32.60	19	643	0.03	0.05740	0.00270	0.32630	0.00169	0.04090	0.00010	258.7	6.4
KG2-12	2.30	246	731	0.34	0.04840	0.00110	0.01160	0.00027	0.00230	0.00004	14.6	2.7
KG2-13 *	26.40	13	358	0.03	0.05950	0.00260	0.52160	0.00237	0.06390	0.00019	399.1	11.5

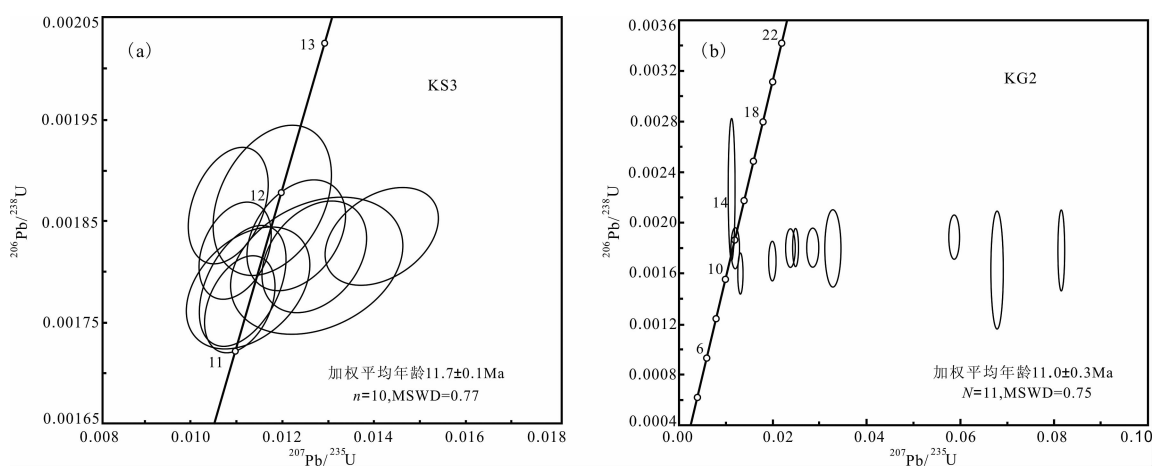


图 7 西昆仑苦子干透辉石正长岩(a)和透辉石花岗岩(b)锆石 U-Pb 年龄谐和图
 Fig. 7 U-Pb concordia diagrams of representative zircons from Kuzigan diopside syenite (a) and diopside granite (b) in western Kunlun

表 4 西昆仑苦子干钾质碱性杂岩体锆石 Lu-Hf 同位素分析结果

Table 4 Lu-Hf isotopic data of zircons from Kuzigan potassio alkaline complex mass in western Kunlun

样品	年龄 (Ma)	$^{176}\text{Yb}/^{177}\text{Hf}$	$^{176}\text{Lu}/^{177}\text{Hf}$	$^{176}\text{Hf}/^{177}\text{Hf}$	2σ	$^{176}\text{Hf}/^{177}\text{Hf}_{\text{i}}$	$\epsilon_{\text{Hf}}(0)$	$\epsilon_{\text{Hf}}(t)$	$T_{\text{DM1}}(\text{Ma})$	$T_{\text{DM2}}(\text{Ma})$	$f_{\text{Lu/Hf}}$
透辉石正长岩											
KS3-1	11.7	0.038594	0.001025	0.282525	0.000012	0.282524	-8.7	-8.5	1031	1639	-0.97
KS3-2	11.7	0.029426	0.000770	0.282548	0.000010	0.282548	-7.9	-7.7	991	1586	-0.98
KS3-3	11.7	0.034800	0.000900	0.282610	0.000011	0.282610	-5.7	-5.5	908	1448	-0.97
KS3-4	11.7	0.011638	0.000318	0.282581	0.000010	0.282581	-6.7	-6.5	933	1511	-0.99
KS3-5	11.7	0.055660	0.001498	0.282597	0.000012	0.282597	-6.2	-5.9	940	1476	-0.95
KS3-6	11.7	0.029517	0.000784	0.282558	0.000009	0.282558	-7.6	-7.3	977	1563	-0.98
KS3-7	11.7	0.060933	0.001673	0.282559	0.000011	0.282559	-7.5	-7.3	999	1561	-0.95
KS3-8	11.7	0.041932	0.001122	0.282536	0.000012	0.282536	-8.3	-8.1	1017	1614	-0.97
KS3-9	11.7	0.047440	0.001207	0.282576	0.000011	0.282576	-6.9	-6.7	962	1523	-0.96
KS3-10	11.7	0.044230	0.001133	0.282584	0.000011	0.282584	-6.6	-6.4	950	1505	-0.97
KS3-11	11.7	0.015689	0.000410	0.282573	0.000009	0.282572	-7.1	-6.8	948	1531	-0.99
透辉石花岗岩											
KG2-1	11.0	0.021416	0.000762	0.282541	0.000007	0.282541	-8.2	-7.9	1000	1602	-0.98
KG2-2	11.0	0.043073	0.001319	0.282540	0.000011	0.282540	-8.2	-8.0	1017	1605	-0.96
KG2-3	11.0	0.017745	0.000577	0.282530	0.000010	0.282530	-8.6	-8.3	1011	1627	-0.98
KG2-4	11.0	0.031957	0.001053	0.282572	0.000007	0.282572	-7.1	-6.8	964	1532	-0.97
KG2-5	11.0	0.022619	0.000778	0.282506	0.000008	0.282506	-9.4	-9.2	1049	1681	-0.98
KG2-6	11.0	0.011328	0.000371	0.282524	0.000009	0.282524	-8.8	-8.5	1015	1642	-0.99
KG2-7	11.0	0.012328	0.000459	0.282561	0.000010	0.282561	-7.5	-7.2	966	1559	-0.99
KG2-8	11.0	0.006697	0.000205	0.282553	0.000007	0.282553	-7.7	-7.5	970	1576	-0.99
KG2-9	11.0	0.018571	0.000681	0.282532	0.000011	0.282532	-8.5	-8.3	1011	1623	-0.98
KG2-10	11.0	0.018841	0.000639	0.282528	0.000008	0.282527	-8.6	-8.4	1016	1633	-0.98

注: $\epsilon_{\text{Hf}}(0) = ((^{176}\text{Hf}/^{177}\text{Hf})_{\text{S}} / (^{176}\text{Hf}/^{177}\text{Hf})_{\text{CHUR},0} - 1) * 10000$, $f_{\text{Lu/Hf}} = (^{176}\text{Hf}/^{177}\text{Hf})_{\text{S}} / (^{176}\text{Hf}/^{177}\text{Hf})_{\text{CHUR}} - 1$, $\epsilon_{\text{Hf}}(t) = ((^{176}\text{Hf}/^{177}\text{Hf})_{\text{S}} - (^{176}\text{Lu}/^{177}\text{Hf})_{\text{S}} * (e^{\lambda t} - 1)) / ((^{176}\text{Hf}/^{177}\text{Hf})_{\text{CHUR},0} - (^{176}\text{Lu}/^{177}\text{Hf})_{\text{CHUR}} * (e^{\lambda t} - 1) - 1) * 10,000$, $T_{\text{DM1}}(\text{Hf}) = \lambda / \lambda * (1 + (^{176}\text{Hf}/^{177}\text{Hf})_{\text{S}} - (^{176}\text{Hf}/^{177}\text{Hf})_{\text{DM}}) / ((^{176}\text{Lu}/^{177}\text{Hf})_{\text{S}} - (^{176}\text{Lu}/^{177}\text{Hf})_{\text{DM}})$, $T_{\text{DM2}}(\text{Hf}) = T_{\text{DM1}}(\text{Hf}) - (T_{\text{DM1}}(\text{Hf}) - t)((f_{\text{CC}} - f_{\text{S}}) / (f_{\text{CC}} - f_{\text{DM}}))$; where, $(^{176}\text{Lu}/^{177}\text{Hf})_{\text{S}}$ and $(^{176}\text{Hf}/^{177}\text{Hf})_{\text{S}}$ are the measured values of samples; $(^{176}\text{Lu}/^{177}\text{Hf})_{\text{CHUR}} = 0.0332$ and $(^{176}\text{Hf}/^{177}\text{Hf})_{\text{CHUR},0} = 0.282772$ (Blichert-Toft et al., 1997); $(^{176}\text{Lu}/^{177}\text{Hf})_{\text{DM}} = 0.0384$ and $(^{176}\text{Hf}/^{177}\text{Hf})_{\text{DM}} = 0.28325$ (Griffin et al., 2000); $f_{\text{CC}} = -0.548$ (average continental crust), $f_{\text{DM}} = 0.16$, $t = \text{crystallization time of zircon}$, $\lambda = 1.865 * 10^{-11} \text{ yr}^{-1}$ (Söderlund et al., 2004)。

由上可知, 苦子干钾质碱性杂岩体的 $\epsilon_{\text{Hf}}(t)$ 范围在 $-9.2 \sim -5.5$ 之间, 存在较大的变化区间, 反映了岩浆来源可能多样。如图 8 所示, $\epsilon_{\text{Hf}}(t)$ 值介于球粒陨石与下地壳之间, 显示了岩石起源于富集地幔或者下地壳。

4 讨论

4.1 岩石类型

关于苦子干钾质碱性杂岩体的岩石类型, 前人的定名如下: ①英辉正长岩和碱性正长花岗岩(新疆地质矿产局二大队, 1985); ②透辉石正长岩和透辉石花岗岩(Zhang Yuquan et al., 1994); ③细粒斑状霓辉正长岩、中粒等粒霓辉正长岩和花岗岩(Luo Zhaohua et al., 2003); ④霓辉正长岩和透辉石正长花岗岩(Ke Shan et al., 2006); ⑤石英霓辉正长岩、霓辉正长岩和碱性花岗岩(Wang Yawei et al., 2013)。辉石电子探针结果表明, 苦子干钾质碱性杂岩体富碱($\text{Na}_2\text{O} + \text{K}_2\text{O}$)、高钾($\text{Na}_2\text{O}/\text{K}_2\text{O}$)和富

钙(CaO), 岩体中的辉石均表现出富 Ca 贫 Na 的特点。当岩浆结晶的时候, Ca 要比 Na 先进入晶格结晶, Ca 会比 Na 更优先与岩浆中的 Mg、Fe 反应, 当 Ca 相对于 Mg、Fe 不足的时候, Mg、Fe 会相对过剩, 这时候 Na 才有可能与其反应生成霓辉石(Wei Dongliang et al., 2005)。碱性岩中是否出现霓辉石取决于其岩石化学成分, 只有当 Ca 的含量相对较低的时候, 才有可能出现霓辉石。结合电子探针结果, 我们认为在苦子干钾质碱性杂岩体中不会出现霓石、霓辉石和钠闪石等矿物。所以, 苦子干钾质碱性杂岩体的岩石类型为透辉石正长岩和透辉石花岗岩。

4.2 岩体形成时代

关于苦子干钾质碱性杂岩体时代的研究, 从 20 世纪八十年代中期已经开始。这些研究主要使用 K-Ar 和 Ar-Ar 方法, 测得正长岩和花岗岩的年龄范围分别为 $54 \sim 13\text{ Ma}$ 和 $33 \sim 18\text{ Ma}$ (新疆地质矿产局二大队, 1985; Xu Ronghua et al., 1996; Luo

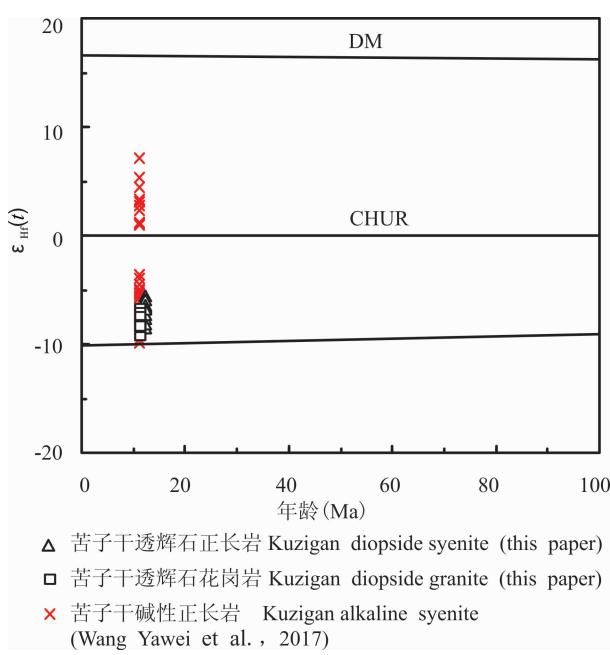


图 8 西昆仑苦子干钾质碱性杂岩体锆石 Hf 同位素
Fig. 8 Zircon Hf isotopic composition of the Kuzigan

potassic alkaline complex mass in western Kunlun
DM 表示亏损地幔演化线, CHUR 表示球粒陨石演化线, LC 表示
下地壳演化线

DM represents the depleted mantle evolution line, CHUR
represents the chondrite evolution line, and LC represents the
lower crust evolution line

Zhaohua et al., 2003)。近年来,随着锆石微区原位 U-Pb 测年技术的广泛应用,我们可以准确地确定侵入岩年龄。之前的研究表明正长岩和花岗岩的年龄范围分别为 11.1~10.46 Ma 和 11.9~10.45 Ma (Ke Shan et al., 2008; Jiang Yaohui et al.,

2012; Wang Yawei et al., 2013)。本文锆石 U-Pb 定年获得透辉石正长岩和透辉石花岗岩年龄值分别为 11.7 ± 0.1 Ma 和 11.0 ± 0.3 Ma, 均属于喜马拉雅期, 相当于中新世末。排除前人因测试方法误差得到的较大年龄, 可以得到苦子干钾质碱性杂岩体的成岩周期在 18~11 Ma, 成岩峰值在 11 Ma 左右。前人研究表明哀牢山-金沙江钾质碱性岩浆岩带在成岩时代上具有东早西晚的特征 (Zhang Yuquan et al., 1987), 苦子干钾质碱性杂岩体位于哀牢山-金沙江钾质碱性岩浆岩带西段, 成岩时代晚于该条岩浆岩带的东部和中部地区。

4.3 岩石成因及岩浆来源

苦子干透辉石花岗岩的主量和微量元素组成类似于 A 型花岗岩 (Whalen et al., 1987)。在花岗岩相关判别图解中 (图 9), 苦子干透辉石花岗岩样品 $10000\text{Ga}/\text{Al}$ 指数介于 2.80~3.17 之间, 明显高于 I 型 (2.1) 和 S 型 (2.28) 花岗岩的平均值, 样品投点均落在 A 型花岗岩内 (Whalen et al., 1987; Eby, 1990)。根据锆石饱和温度的计算公式 { $T_{\text{Zr}} = 12900 / [2.95 + 0.85 \times M + \ln(496000/Zr)_{\text{melt}}]$ }, 计算得出花岗岩的锆石饱和温度介于 851~866°C, 明显高于平均温度的 I 型花岗岩和 S 型花岗岩 (分别为 781°C 和 764°C, King et al., 1997), 与典型的 A 型花岗岩接近 (839°C, King et al., 1997)。因此, 我们认为苦子干透辉石花岗岩属于 A 型花岗岩。

关于 A 型花岗岩的成因, 通常有以下三种模式: ①幔源拉斑质岩浆或碱性岩浆的高度结晶分异 (Turner et al., 1992; Litvinovsky et al., 2002);

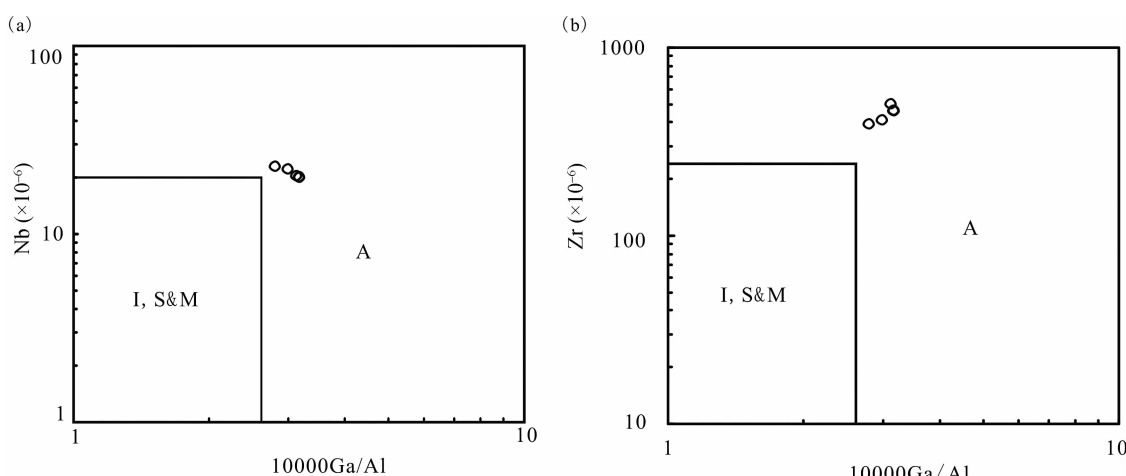


图 9 西昆仑苦子干透辉石花岗岩成因类型判别图解(据 Whalen et al., 1987)

Fig. 9 Discrimination diagrams of diopside granite types in western Kunlun (after Whalen et al., 1987)

②地壳部分熔融 (King et al., 1997; Shellnutt et al., 2011); ③壳源长英质岩浆与幔源铁镁质岩浆混合 (Kemp et al., 2005)。由于苦子干 A 型花岗岩周围没有与之密切相关的基性岩发育, 结合 Nb 亏损, 可以基本排除其由幔源基性物质结晶分异形成的可能性。岩体 SiO_2 含量较高 (>69%), MgO 含量较低 (<0.44%), Ni 、 Co 、 Cr 等相容元素含量也较低, 说明并非直接来源于地幔。透辉石花岗岩 $^{87}\text{Sr}/^{86}\text{Sr}_i$ 介于 0.708741~0.710049 之间 (Ke Shan et al., 2008; Jiang Yaohui et al., 2012), 高于地幔初始 Sr 同位素值 (0.7045, DePaolo et al., 1979), 表明该岩体的源区可能存在壳源物质。花岗岩全岩 $\epsilon_{\text{Nd}}(t)$ 范围为 -8.6~-10.18 (Ke Shan et al., 2008; Jiang Yaohui et al., 2012), 锆石 $\epsilon_{\text{Hf}}(t)$ 范围为 -9.2~-6.8, 且 Hf 的二阶段模式年龄远大于其形成年龄, 表明其受到地壳的混染作用或者来自于富集地幔 (Wu Fuyuan et al., 2007)。此外, 在本次透辉石花岗岩测年中, 获得两颗继承锆石, $^{206}\text{Pb}/^{238}\text{U}$ 年龄分别为 258.7 ± 6.4 Ma 和 399.1 ± 11.5 Ma。结合 Wang Yawei et al. (2013) 测得的五颗继承锆石的年龄 (630 Ma, 630 Ma, 536 Ma, 326 Ma, 85 Ma), 透辉石花岗岩继承锆石年龄变化于 630~85 Ma 之间, 继承性锆石核的存在, 说明地壳部分熔融物质参与了侵入岩的形成过程。苦子干透辉石花岗岩的源区应为上涌的热的软流圈物质混合古老的

下地壳组分。

结合前人数据, 苦子干正长岩和花岗岩的稀土元素配分曲线近乎平行, 稀土含量大致同步变化, 样品均富集 Rb、Ba、Th、U、Sr 等大离子亲石元素, 亏损 Nb、Ta、Zr、Hf、Ti 等高场强元素, 以及表现为弱的负 Eu 异常, 说明两者的物质来源与岩浆演化过程具有相似性。苦子干钾质碱性杂岩体中正长岩 $^{87}\text{Sr}/^{86}\text{Sr}_i$ 介于 0.708129~0.711684 之间, $\epsilon_{\text{Nd}}(t)$ 介于 -8.47~-14.03 之间, 岩体中含有暗色包体 (Wang Yawei et al., 2013), 同样反映了苦子干正长岩具壳幔岩浆混合成因特征 (Zorpi et al., 1989)。综上所述, 苦子干正长岩和正长花岗岩类应是同源不同阶段的产物。

苦子干钾质碱性杂岩体是哀牢山-金沙江新生代钾质碱性岩浆岩带的西延部分 (Zhang Yuquan et al., 1997), 成因与印度和欧亚两大陆碰撞密切相关。由于印度洋中脊继续扩张, 导致青藏高原向北推移, 而受到塔里木和柴达木盆地古老基底的阻挡, 挤压应力方向与喀喇昆仑断裂间的夹角变小 (<45°), 使原先的喀喇昆仑断裂由转换挤压带转变为转换伸展带 (Li Haibing et al., 2006), 形成拉分盆地和张性断裂 (Zheng Xiangshen et al., 1996)。苦子干钾质碱性杂岩体成分投点位于后碰撞花岗岩区, 同样反映了造山作用后期松弛的伸展环境 (图 10, Pearce et al., 1984, 1996)。Matte et al. (1996)

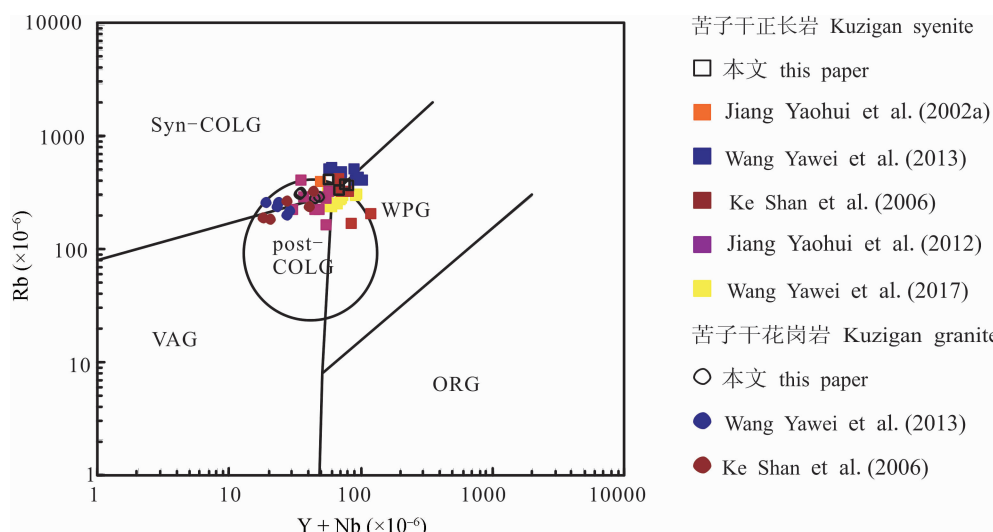


图 10 苦子干钾质碱性杂岩体构造环境判别图解(据 Pearce et al., 1984, 1996)

Fig. 10 Discrimination diagrams of tectonic setting for the Kuzigan potassio alkaline complex mass
(after Pearce et al., 1984, 1996)

ORG—洋脊花岗岩; WPG—板内花岗岩; VAG—火山弧花岗岩; syn-COLG—同碰撞花岗岩; post-COLG—后碰撞花岗岩
ORG—Oceanic ridge granites; WPG—within plate granites; VAG—volcanic arc granites;
syn-COLG—syn-collisional granites; post-COLG—post-collisional granites

和 Murphy et al. (2000, 2002) 认为喀喇昆仑断裂在~13Ma 和 11Ma 以来发生了右旋剪切活动; 在塔什库尔干断裂地表形成类似盐壳的结晶物, 并发育拉分盆地, 显示了左行走滑断裂的性质 (Liu Dongliang et al., 2011)。印度大陆与欧亚大陆发生碰撞也使得喀喇昆仑地区岩石圈大幅度缩短并加厚, 引发加厚岩石圈发生拆沉作用, 从而引起软流圈物质上涌 (Bao Peisheng et al., 2006)。这些高温岩浆的底侵, 诱发了加厚下地壳物质发生重熔, 并发生混合, 导致钾质碱性岩浆形成。喀喇昆仑断裂带为这些岩浆的上升、就位提供了通道, 伴随地壳的拉张和抬升 (England et al., 1989; Kay et al., 1993), 形成苦子干钾质碱性杂岩体。

5 结论

(1) 锆石 U-Pb 年龄结果显示, 先侵入的透辉石正长岩成岩年龄为 11.7 Ma、后侵入的透辉石花岗岩成岩年龄为 11.0 Ma, 均属于喜马拉雅期, 相当于中新世末。

(2) 苦子干钾质碱性杂岩体中赋存的透辉石和钙铁辉石, 均属于钙质辉石。

(3) 苦子干钾质碱性杂岩体富碱 ($\text{Na}_2\text{O} + \text{K}_2\text{O} = 9.12\% \sim 12.55\%$)、高钾 ($\text{Na}_2\text{O}/\text{K}_2\text{O} = 0.39 \sim 0.76$) 和富钙 ($\text{CaO} = 1.62\% \sim 9.77\%$), 富集 Rb、Ba、Th、U 等大离子亲石元素, 亏损 Nb、Ta、Zr、Hf 和 Ti 等高场强元素, 存在微弱的铕负异常。

(4) 加厚的岩石圈拆沉作用引起软流圈物质上涌底侵, 导致加厚下地壳物质的重熔, 伴随地壳的拉张和抬升, 最终形成苦子干钾质碱性杂岩体。

致谢: 北京离子探针中心的刘敦一研究员、王彦斌研究员和中国科学院广州地球化学研究所同位素地球化学国家重点实验室涂湘林高级工程师协助 U-Pb 年龄测定并提出了许多宝贵的意见, 在此表示衷心的感谢!

References

- Andersen T. 2002. Correction of common lead in U-Pb analyses that do not report ^{204}Pb . *Chemical Geology*, 192(1): 59~79.
- Arnaud N O, Vidal P H, Tapponnier P, Matte P H, Deng Wanming. 1992. The high K_2O volcanism of northwestern Tibet: geochemistry and tectonic implications. *Earth & Planetary Science Letters*, 111: 351~367.
- Bao Peisheng, Xiao Xuchang, Su Li. 2006. Geochemical characteristics of the Potassic volcanics in the northwestern Tibet Plateau and its implications. *Acta Geologica Sinica*, 80 (10): 1578~1587 (in Chinese with English abstract).
- Black L P, Kamo S L, Williams I S, Mundil R, Davis D W, Korsch R J, Foudoulis C. 2003. The application of SHRIMP to Phanerozoic geochronology: a critical appraisal of four zircon standards. *Chemical Geology*, 200(1): 171~188.
- Blichert T J, Albarede F. 1997. The Lu-Hf isotope geochemistry of chondrites and the evolution of the mantle-crust system. *Earth and Planetary Science Letters*, 148(1~2): 243~258.
- Compston W, Williams I S, Kirschvink J L, Zichao Z, Guogang M A. 1992. Zircon U-Pb ages for the Early Cambrian time-scale. *Journal of Geological Society*, 149: 171~184.
- Dai Jingen, Wang Chengshan, Hourigan Jeremy, Li Zhijun, Zhuang Guangsheng. 2013. Exhumation history of the Gangdese batholith, southern Tibetan Plateau: evidence from apatite and zircon (U-Th)/He thermochronology. *The Journal of Geology*, 121: 155~172.
- Depaolo D J, Wasserburg G J. Petrogenetic mixing models and Nd-Sr isotopic patterns. *Geochimica et Cosmochimica Acta*, 1979, 43(4): 615~627.
- England P C, Houseman G A. 1989. Extension during continental convergence, with application to the Tibetan Plateau. *Journal of Geophysical Research: Solid Earth*, B12: 17561~17579.
- Guo Zhengfu, Wilson M, Zhang Lihong, Zhang Maoliang, Cheng, Zhihui, Liu Jiaqi. 2014. The role of subduction channel mélanges and convergent subduction systems in the petrogenesis of post-collisional K-rich mafic magmatism in NW Tibet. *Lithos*, 198~199: 184~201.
- Hou Zengqian, Zhang Hongrui, Pan Xiaofei, Yang Zhiming. 2011. Porphyry Cu(-Mo-Au) deposits related to melting of thickened mafic lower crust: examples from the eastern Tethyan metallogenic domain. *Ore Geology Reviews*, 39: 21~45.
- Irvine T N, Barager W R A. 1971. A guide to the chemical classification of the common volcanic rocks. *Canadian Journal of Earth Sciences*, 8: 523~548.
- Jian Ping, Kröner A, Zhou Gaozhi. 2012. SHRIMP zircon U-Pb ages and REE partition for high-grade metamorphic rocks in the North Dabie complex: Insight into crustal evolution with respect to Triassic UHP metamorphism in east-central China. *Chemical Geology*, 328(11): 49~69.
- Jiang Yaohui, Jiang Shaoyong, Ling Hongfei, Zhou Xunruo, Rui Xingjian, Yang Wanzhi. 2002a. Petrology and geochemistry of shoshonitic plutons from the western Kunlun orogenic belt, Xinjiang, northwestern China: implications for granitoid genesis. *Lithos*, 63(3~4): 165~187.
- Jiang Yaohui, Ling Hongfei, Jiang Shaoyong, Zhou Xunruo, Rui Xingjian, Yang Wanzhi. 2002b. Enrichment of mantle-derived fluids in the formation process of granitoids: evidence from the Himalayan granitoids around Kunlun in the western Qinghai-Tibet Plateau. *Acta Geologica Sinica(English Edition)*, 76(3): 343~350.
- Jiang Yaohui, Liu Zheng, Jia Ruya, Liao Shiyong, Zhou Qing, Zhao Peng. 2012. Miocene potassio-syenite association in western Tibetan Plateau: Implications for shoshonitic and high Ba-Sr granite genesis. *Lithos*, 134~135: 146~162.
- Kay R W, Mahlburg Kay S. 1993. Delamination and delamination magmatism. *Tectonophysics*, 219: 177~189.
- Ke Shan, Luo Zhaohua, Mo Xuanxue. 2006. Mineralogy of Taxkorgan Cenozoic alkaline complex in Xinjiang and its implication to pluton genesis. *Acta Petrologica et Mineralogica*, 25(2): 149~156 (in Chinese with English abstract).
- Ke Shan, Luo Zhaohua, Mo Xuanxue, Zhang Wenhui, Liang Tao, Zhan Huaming. 2008. The geochronology of Taxkorgan alkalic complex, Pamir syntax. *Acta Petrologica Sinica*, 24(2): 315~324 (in Chinese with English abstract).
- Kemp A I S, Wormald R J, Whitehouse M J, Price R C. 2005. Hf isotopes in zircon reveal contrasting sources and crystallization histories for alkaline to peralkaline granites of Temora, southeastern Australia. *Geology*, 33: 797~800.
- King P L, White, A J R, Chappell B, Allen C M. 1997. Characterization and origin of aluminous A-type granites from the Lachlan Fold Belt, Southeastern Australia. *Journal of Petrology*, 38: 371~391.

- Li Congying, Zhang Hong, Wang Fangyue, Liu Jiqiang, Sun Yali, HaoXiluo, Li Yiliang, Sun Weidong. 2012. The formation of the Dabaoshan porphyry molybdenum deposit induced by slab rollback. *Lithos*, 150(5): 101~110.
- Li Haibing, Valli F, Xu Zhiqin, Yang Jingsui, Tapponnier P, Lacassin R, Chen Songyong, Qi Xuexiang, Chevalier M L. 2006. Deformation and tectonic evolution of the Karakorum fault, western Tibet, *Geology in China*, 33(2): 239~255 (in Chinese with English abstract).
- Li Xianhua, Long Wengguo, Li Qiuli, Liu Yu, Zheng Yongfei, Yang Yueheng, Chamberlain K R, Wan Defang, Guo Cunhua, Wang Xuance, Tao Hua. 2010. Penglai Zircon Megacrysts: A potential new working reference material for microbeam determination of Hf-O isotopes and U-Pb Age. *Geostandards and Geoanalytical Research*, 34(2): 117~134.
- Li Xianhua, Qi Changshi, Liu Ying, Liang Xirong, Tu Xianglin, Xie Liewen, Yang Yueheng. 2005. Petrogenesis of the Neoproterozoic bimodal volcanic rocks along the western margin of the Yangtze Block: New constraints from Hf isotopes and Fe/Mn ratios. *Chinese Science Bulletin*, 50: 2481~2486.
- Lin Qingcha, Xia Bin, Zhang Yuquan. 2006. Ar-Ar dating of potassio alkali-rocks in the western Kunlun-Kalakorum mountains-example for the rocks of Yanghu, Zankan and Kuzigan. *Journal of Mineralogy and Petrology*, 26(2): 66~70 (in Chinese with English abstract).
- Litvinovsky B A, Jahn, B M, Zavvilevich, A N, Saunders A, Poula S, Kuzmin D V, Reichow M K, Titov A V. 2002. Petrogenesis of syenite-granite suites from the Bryansk complex (Transbaikalia, Russia): implications for the origin of A-type granitoid magmas. *Chemical Geology*, 189: 105~133.
- Liu Dongliang, Li Haibing, Pan Jiawei, Chevalier M L, Pei Junling, Sun Zhiming, Si Jialiang, Xu Wei. 2011. Morphotectonic study from the northeastern margin of the Pamir to the West Kunlun range and its tectonic implications. *Acta Petrologica Sinica*, 27 (11): 3499~3512 (in Chinese with English abstract).
- Liu Yin, Liu Haichen, Li Xianhua. 1996. Simultaneous precise determination of 40 trace elements in rock samples using ICP-MS. *Geochimica*, 25(6): 552~558 (in Chinese with English abstract).
- Liu Yongsheng, Hu Zhaochu, Gao Shan, Gunther D, Xu Juan, Gao Changgui. 2008. In situ analysis of major and trace elements of anhydrous minerals by LA-ICP-MS without applying an internal standard. *Chemical Geology*, 257: 34~43.
- Lu Yongjun, Kerrich R, McCuaig T, Li Zhengxiang, Hart C J R, Cawood P A, Hou Zengqian, Bagas L, Cliff J, Belousova E A, Tang Suohan. 2013. Geochemical, Sr-Nd-Pb and zircon Hf-O isotopic compositions of Eocene-Oligocene shoshonitic and potassio adakite-like felsic intrusions in Western Yunnan, SW China; Petrogenesis and tectonic implications. *Journal of Petrology*, 54: 1309~1348.
- Ludwing K R. 2003. User's manual for isoplots 3.0: a geochronological toolkit for Microsoft Excel. Berkeley Geochronological Center, Special Publication, 4:1~71.
- Luo Zhaohua, Mo Xuanxue, Ke Shan. 2003. Ages of Taxkorgan alkaline intrusive complex and their geological implications. *Xinjiang Geology*, 21(1), 46~50 (in Chinese with English abstract).
- Matte P, Tapponnier P, Arnaud N, Bourjot L, Avouac J P, Vidal P, Liu Qing, Pan Yusheng, Wang Yi. 1996. Tectonics of western Tibet, between the Tarim and the Indus. *Earth and Planetary Science Letters*, 142(3~4): 311~330.
- Morimoto N. 1988. Nomenclature of pyroxenes. *Mineralogical Magazine*, 52: 431~435.
- Murphy M A, Yin An, Kapp P. 2000. Southward propagation of the Karakoram fault system, southwest Tibet: timing and magnitude of slip. *Geology*, 28: 451~454.
- Murphy M A, Yin An, Kapp P. 2002. Structural evolution of the Gurla Mandata detachment system, southwest Tibet: implications for the eastward extent of the Karakoram fault system. *Geological Society of America Bulletin*, 114: 428 ~447.
- Nowell G M, Kempton P D, Noble S R, Fitton J G, Saunders A D, Mahoney J J, Taylor R N. 1998. High precision Hf isotope measurements of MORB and OIB by thermal ionisation mass spectrometry: insights into the depleted mantle. *Chemical Geology*, 149(3~4): 211~233.
- Patchett P J, Tatsumoto M. 1981. A routine high-precision method for Lu-Hf isotope geochemistry and chronology. *Contributions to Mineralogy and Petrology*, 75(3): 263~267.
- Pearce J A. 1996. Sources and settings of granitic rocks. *Episodes*, 19: 120~125.
- Pearce J A, Harris, N B W, Tindle, A G. 1984. Trace element discrimination diagrams for the Tectonic Interpretation of granitic rocks. *Journal of Petrology*, 25: 956~983.
- Shellnutt J G, Jahn B M, Zhou Meifu. 2011. Crustally-derived granites in the Panzhihua region, SW China: Implications for felsic magmatism in the Emeishan large igneous province. *Lithos*, 123: 145~157.
- Sun S S, McDonough W F. 1989. Chemical and isotopic systematics of oceanic of oceanic basalts: implications for mantle composition and processes. *Geological Society of London, Special Publications*, 42: 313~345.
- Tran M D, Liu Junlai, Nguyen Q L, Chen Yue, Tang Yuan, Song Zhipie, Zhang Zhaochong, Zhao Zhidan. 2014. Cenozoic high-K alkaline magmatism and associated Cu-Mo-Au mineralization in the Jinping-Fan Si Pan region, southeastern Ailao Shan-Red River shear zone, southwestern China-northwestern Vietnam. *Journal of Asian Earth Sciences*, 79(2): 858~872.
- Turner S P, Foden J D, Morrison, R S. 1992. Derivation of some A-type magmas by fractionation of basaltic magma; an example from the Padthaway Ridge, South Australia. *Lithos*, 28: 151~179.
- Wang Erchie, Kamp Peter J J, Xu Ganqing, Hodges Kip V, Meng Kai, Chen Lin, Wang Gang, LuoHui. 2015. Flexural bending of southern Tibet in a retro-foreland setting. *Scientific Reports*, 5: 12076.
- Wang Liankui, Xia Bin, Zhang Yuquan, Chen Genwen. 2003. A humble opinion on the "Potassio and sodic two mantle alkali-rich magma systems". *Geological Journal of China Universities*, 9 (4): 545~555 (in Chinese with English abstract).
- Wang Yawei, Liao Xiaoyin, Liu Liang, Xiao Peixi, Cao Yuting, Yang Wenqiang, Kang Lei, Liang Sha. 2013. Petrogenesis and tectonic implications of the Cenozoic alkaline complex in Kuzigan, Taxkorgan, west Kunlun. *Northwestern Geology*, 46 (4), 1~24 (in Chinese with English abstract).
- Wang Yawei, Zhang Li, Zhu Yixiang. 2017. Petrogenesis of alkaline syenite from the Kuzigan, (Taxkorgan, West Kunlun); evidence from the bulk geochemical composition and mineral geochemistry. The first youth BBS academic proceedings excellent of geological science and technology in Yunnan province (in Chinese with English abstract).
- Whalen J B, Currie, K L, Chappel, B W. 1987. A-type granites: geochemical characteristics, discrimination and petrogenesis. *Contributions to Mineralogy and Petrology*, 95: 407~419.
- Wei Dongliang, Xia Bin, Zhang Yuquan, Wang Ran, Wan Shaokai. 2005. The pyroxenes composition and petrochemical characteristics of Zhuopan-Liuhe alkali rock bodies in western Yunnan province, China. *Journal of Mineralogy and Petrology*, 25(2): 15~19 (in Chinese with English abstract).
- Williams H M, Turner S P, Peace J A, Kelley S P, Harris N B W. 2004. Nature of the source regions for post-collisional, potassio magmatism in southern and northern Tibet from geochemical variations and inverse trace element modelling. *Journal of Petrology*, 45: 555~607.
- Williams I S, Buick I S, Cartwright I. 1996. An extended episode of early Mesoproterozoic metamorphic fluid flow in the Reynolds Range, central Australia. *Journal of Metamorphic Geology*, 14 (1): 29~47.

- Wright J B. 1969. A simple alkalinity ratio and its application to questions of non-orogenic granite genesis, Geological Magazine, 106: 307~384.
- Wu Fuyuan, Li Xianhua, Zheng Yongfei, Gao Shan. 2007. Lu-Hf isotopic systematics and their applications in petrology. Acta Petrologica Sinica, 23: 185~220 (in Chinese with English abstract).
- Wu Fuyuan, Liu Chuanzhou, Zhang Liangliang, Zhang Chang, Wang Jiangang, Ji Weiqiang, Liu Xiaochi. 2014. Yarlung Zangbo ophiolite: a critical updated view. Acta Petrologica Sinica, 30(2): 293~325 (in Chinese with English abstract).
- Xia Bin, Lin Qingcha, Zhang Yuquan, Liang Huaying, Xu Lifeng, Li Jianfeng, Wang Yanbin. 2009. SHRIMP U-Pb Dating of zircon from gneiss in the Tongmai Region: evidence for the India-Eurasia collision time. Acta Geologica Sinica, 83(3): 347~352 (in Chinese with English abstract).
- Xia Bin, Lu Ye, Yuan Yuanjuan, Chen Weiyuan, Zhang Xiao, Xu Chi, Yu Shengrui, Wan Zhifeng. 2018. Mixing of enriched lithospheric mantle-derived and crustal magmas: evidence from the Habo Cenozoic Porphyry in Western Yunnan. Acta Geologica Sinica (English Edition), 92: 1753~1768.
- Xu Leiluo, Bi Xianwu, Hu Ruizhong, Zhang Xingchun, Su Wenchao, Qu Wenjun, Hu Zhaochu, Tang Yongyong. 2012. Relationships between porphyry Cu-Mo mineralization in the Jinshajiang-Red River metallogenic belt and tectonic activity: Constraints from zircon U-Pb and molybdenite Re-Os geochronology. Ore Geology Reviews, 48: 460~473.
- Xu Ronghua, Zhang Yuquan, Xie Yingwen. 1996. Isotopic geochemistry of plutonic rocks. Geological evolution of the Karakorum and Kunlun Mountains. Beijing: Seismological Press, 137~186.
- Xu Zhiqin, Dilek Y, Yang Jingsui, Liang Fenghua, Liu Fei, Ba Dengzhu, Cai Zihui, Li Guangwei, Dong Hanwen, Ji Shaoheng. 2015. Crustal structure of the Indus-Tsangpo suture zone and its ophiolites in southern Tibet. Gondwana Research, 27(2): 507~524.
- Yin An, Harrison T M. 2000. Geologic evolution of the Himalayan-Tibetan orogen. Annual Review of Earth and Planetary Sciences, 28(1): 211~280.
- Yuan Yajuan, Xia Bin, Zhang Yuquan, Xia Lianze, Li He. 2013. Geochemistry and zircon U-Pb ages of the potassio alkalic rocks at Nangqian county, Qinghai province. Geological Journal of China Universities, 19(4): 611~619 (in Chinese with English abstract).
- Zhang Kaijun, Xia Bin, Zhang Yuxiu, Liu Weieliang, Zeng Lu, Li Jianfeng, Xu Lifeng. 2014. Central Tibetan Meso-Tethyan oceanic plateau. Lithos, 210~211: 278~288.
- Zhang Yuquan, Xie Yingwen. 1997. Geochronology and Nd, Sr isotopic features of alkalic-rich intrusive rocks along the Ailaoshan-Jinshajiang belt. Science in China Series D, 27: 289~293.
- Zhang Yuquan, Xie Yingwen. 1994. Alkali-rich intrusive rocks in the Qinghai-Xizang Plateau and its vicinities as exemplified by Kuganzi and Taihe plutons. Science in China (Series B), 24(10): 1102~1108 (in Chinese).
- Zhang Yuquan, Xie Yingwen, Tu Guangzhi. 1987. Preliminary studies of the alkali-rich intrusive rocks in the Ailaoshan-Jinshajiang belt and their bearing on rift tectonics. Acta Petrologica Sinica, 2(1): 17~25 (in Chinese with English abstract).
- Zhang Yuxiu, Zeng Lu, Li Zhiwu, Wang Chengshan, Zhang Kaijun, Yang Wenguang, Guo Tonglou. 2015. Late Permian-Triassic siliciclastic provenance, palaeogeography, and crustal growth of the Songpan terrane, eastern Tibetan Plateau: evidence from U-Pb ages, trace elements, and Hf isotopes of detrital zircons. International Geology Review, 57: 159~181.
- Zheng Xiangshen, Bian Qiantao, Zheng Jiankang. 1996. On the Cenozoic volcanic rocks in HOH Xil district, Qinghai Province. Acta Petrologica Sinica, 12(4): 530~545 (in Chinese with English abstract).
- Zhong Dalai, Ding Lin. 1996. A discussion on uplift process and mechanism of Tibetan Plateau. Science in China (Series D), 26(4): 289~295 (in Chinese).
- Zorpi M J, Coulon C, Orsini J B, Cocotta C. 1989. Magma mingling, zoning and emplacement in cal-alkaline granitoid plutons. Tectonophysics, 157: 315~329.
- ## 参 考 文 献
- 鲍佩声,肖序常,苏犁. 2006. 西藏高原西北缘钾质火山岩地球化学特征及其地质涵义. 地质学报,80(10): 1578~1587.
- 柯珊,罗照华,莫宣学,张文会,梁涛,詹华明. 2008. 帕米尔构造结塔什库尔干碱性杂岩同位素年代学研究. 岩石学报,24(2): 315~324.
- 柯珊,罗照华,莫宣学. 2006. 塔什库尔干新生代碱性杂岩造岩矿物化学分析及成因意义. 岩石矿物学杂志,25(2): 149~156.
- 李海兵, Franck Valli, 许志琴, 杨经绥, Paul Tapponnier, Robin Lacassin, 陈松永, 戚学祥, Marie-Luce Chevalier. 2006. 喀喇昆仑断裂的变形特征及构造演化. 中国地质,33(2): 239~255.
- 林清茶,夏斌,张玉泉. 2006. 西昆仑-喀喇昆仑地区钾质碱性岩Ar-Ar年龄—以羊湖、普央和苦子干岩体为例. 矿物岩石,26(2): 66~70.
- 刘栋梁,李海兵,潘家伟,Chevalier Marie-luce,裴军令,孙知明,司家亮,许伟. 2011. 帕米尔东北缘-西昆仑的构造地貌及其构造意义. 岩石学报,27(11): 3499~3512.
- 刘颖,刘海臣,李献华. 1996. 用ICP-MS准确测定岩石样品中的40余种微量元素. 地球化学,25(6): 552~558.
- 罗照华,莫宣学,柯珊. 2003. 塔什库尔干碱性杂岩体形成时代及其地质意义. 新疆地质,21(1): 46~50.
- 王联魁,夏斌,张玉泉,陈根文. 2003. 研究“钾质和钠质两个地幔富碱岩浆体系”的刍议. 高校地质学报,9(4): 545~555.
- 王亚伟,廖小莹,刘良,校培喜,曹玉亭,杨文强,康磊,梁莎. 2013. 西昆仑塔什库尔干苦子干碱性杂岩体的成因及其构造意义. 西北地质,46(4): 1~24.
- 王亚伟,张力,朱毅翔. 2017. 西昆仑塔什库尔干苦子干碱性正长岩成因—来自全岩和矿物地球化学的证据. 云南省首届青年地质科技论坛优秀学术论文集.
- 韦栋梁,夏斌,张玉泉,王冉,万哨凯. 2005. 滇西卓潘-六合碱性岩的辉石成分及其岩石化学特征. 矿物岩石,25(2): 15~19.
- 吴福元,李献华,郑永飞,高山. 2007. Lu-Hf同位素体系及其岩石学应用. 岩石学报,23: 185~220.
- 吴福元,刘传周,张亮亮,张畅,王建刚,纪伟强,刘小驰. 2014. 雅鲁藏布蛇绿岩——事实与臆想. 岩石学报,30(2): 293~325.
- 夏斌,林清茶,张玉泉,梁华英,徐力峰,李建峰,王彦斌. 2009. 印度与欧亚两大陆块碰撞时间的厘定:来自锆石SHRIMP U-Pb年龄的证据. 地质学报,83(3): 347~352.
- 新疆地质矿产局二大队. 1985. 新疆南疆西部1/50万地质图及说明书. 北京:地质出版社,251~361.
- 袁亚娟,夏斌,张玉泉,夏连泽,李贺. 2013. 青海省囊谦县钾质碱性岩地球化学特征和锆石U-Pb年龄. 高校地质学报,19(4): 611~619.
- 张玉泉,谢应雯,涂光炽. 1987. 哀牢山-金沙江富碱侵入岩及其与裂谷构造关系初步研究. 岩石学报,2(1): 17~25.
- 张玉泉,谢应雯. 1994. 青藏高原及邻区富碱侵入岩—以苦子干和太和二岩体为例. 中国科学(B辑),24(10): 1102~1108.
- 郑祥身,边千韬,郑健康. 1996. 青海可可西里地区新生代火山岩研究. 岩石学报,12(4): 530~545.
- 钟大赉,丁林. 1996. 青藏高原的隆起过程及其机制探讨. 中国科学(D辑),26(4): 289~295.

Geochemical characteristics and geochronology of the Cenozoic diopside syenite and diopside granite from Kuzigan, Western Kunlun area

YUAN Yajuan¹⁾, CHEN Weiyan^{* 2)}, XIA Bin³⁾, ZHANG Yuquan⁴⁾, XIAO Jinguo¹⁾, ZHOU Houyun¹⁾

1) School of Geography, South China Normal University, Guangzhou, 510631;

2) Research Institute of Petroleum Exploration and Development, PetroChina, Beijing, 100083;

3) School of Marine Sciences, Sun Yat-sen University, Guangzhou, 510275;

4) Guangzhou Institute of Geochemistry, Chinese Academy of Sciences, Guangzhou, 510640

* Corresponding author: 7104700@qq.com

Abstract

Kuzigan potassic alkaline complex mass is composed of alkali syenite and granite. Syenite is mainly composed of potassium feldspar and diopside, while granite is composed of potassium feldspar, plagioclase, quartz and diopside. The pyroxenes in the rocks are identified as calcium pyroxene, including diopside and hedenbergite. Petrogeochemical analysis shows that these rocks belong to potassic alkaline series with high alkali, potassium and calcium. Moreover, the rocks are enriched in the large-ion lithophile elements (LILE, Rb, Ba, Th, U and Sr) and Pb, but depleted in high field strength elements (HFSE, Nb, Ta, Zr, Hf and Ti). Rare earth element (REE) content ranges from 372.37×10^{-6} to 1218.07×10^{-6} . The ratio of LREE/HREE is relatively high (21~37), and weak Eu negative anomalies ($\text{Eu}/\text{Eu}^* = 0.66 \sim 0.84$). Systematic LA-ICP-MS and SHRIMP U-Pb zircon dating results indicate ages of diopside syenite and diopside granite are 11.7 ± 0.1 Ma and 11.0 ± 0.3 Ma, respectively, which belong to the Himalayan period, equivalent to the end of the Miocene. The $\epsilon_{\text{Hf}}(t)$ values of the zircons from the two types of rock range from -9.4 to -5.5, which plot between those of chondrite and the lower crust. The results show that the collision between the Indian continent and the Eurasian continent caused the lithosphere in the West Kunlun and Karakoram area to be shortened and greatly thickened, leading to the delamination of the thickened lithosphere and the upwelling of the asthenosphere material and the remelting of the thickened lower crust material. With the extension and uplift of the crust, Kuzigan potassic alkaline complex mass was formed.

Key words: geochemistry; zircon U-Pb age; zircon Hf isotope; potassic alkaline complex; Kuzigan